J. Synchrotron Rad. (1997). **4**, 163–168

Synchrotron Radiation Study of the Relation between Structure and Strain in Polyurethane Elastomers

D. C. Creagh,[a] P. M. O'Neill[b] and D. J. Martin[c]

[a]Faculty of Information Science and Engineering, University of Canberra, PO Box 1, Belconnen, ACT 2616, Australia, [b]School of Physics, University College, The University of New South Wales, Australian Defence Force Academy, Canberra, ACT 2600, Australia, and [c]CRC for Cardiac Technology, Graduate School of Biomedical Engineering, University of New South Wales, Sydney, NSW 2052, Australia. E-mail: dudleyc@ise.canberra.edu.au

(*Received 3 September 1996; accepted 24 February 1997*)

This paper describes a system for the study of the relation between structure and applied strain in thermoplastic polyurethane elastomers using the Australian National Beamline Facility at the Photon Factory, KEK, Tsukuba, Japan. The system uses the sagittal focusing monochromator at beamline 20B to provide a high-intensity focused beam which then falls on the specimen mounted in a miniature tensometer mounted in the unique vacuum diffractometer (BIGDIFF). Imaging plates were used to record simultaneously SAXS and WAXS patterns from the specimen at a particular strain. The change in SAXS and WAXS patterns with loading and unloading was recorded using a ten-plate imaging-plate changer.

Keywords: WAXS; SAXS; X-ray fibre diffraction; polyurethane; morphology.

1. Introduction

X-ray fibre diffraction is used extensively to characterize the structural changes induced in polymers by applied stress. It is conventional to consider the scattering from these specimens as wide-angle X-ray scattering (WAXS) if the scattering is caused by electron-density variations which cause scattering at angles greater than 2°, and as small-angle X-ray scattering (SAXS) if the scattering angles are less than 2°, for an incident wavelength of *e.g.* 1.5405 Å. This distinction is somewhat arbitrary, and has been determined in the past by the characteristics of the X-ray cameras used to record the data. Modern area detectors give experimentalists the opportunity to record data for both the SAXS and the WAXS regions simultaneously. A recent paper by Hughes *et al.* (1996) described the use of CCD cameras to study simultaneously time-resolved SAXS/WAXS from polyethylene as it was drawn at rates of up to 7200% min^{-1}, and for temperatures from ambient up to 623 K. Others (Bras *et al.*, 1995; Butler *et al.*, 1995) have used two-dimensional gas-filled area detectors to collect the SAXS/WAXS or the WAXS patterns from deformed polymers. The gas-filled detector systems have deficiencies, the principal of which are lack of resolution, the count rate interdependence of all elements of the detector system, and parallax.

O'Neill (1996) has used a two-dimensional gas-filled detector for SAXS/WAXS studies of polyurethane elastomers, but the resolution achievable from this laboratory-based system is inadequate for the proper characterization of the strain dependence of the structure of these elastomers. In the event, studies of SAXS only were possible, and the time taken to acquire data was approximately 2 h per increment in strain. Clearly relaxation processes can take place in this time. Despite this deficiency, O'Neill was able to observe the development of the SAXS pattern from a circularly symmetric shape at 0% strain to a peanut shape lying parallel to the direction of applied stress at 320% strain.

Imaging plates have been used for the study of polymer fibre patterns. In a recent paper Suehiro *et al.* (1996) have studied the dynamic changes to the SAXS pattern of a polymer which was subjected to an oscillatory shear stress, using imaging plates to record the SAXS patterns from a synchrotron radiation source (the Photon Factory) with minimum exposure times of 0.5 s. The area of the SAXS pattern was $100 \times 100\ mm^2$. By using a beam shutter and moving the imaging plate after exposure they were able to produce stroboscopic representations of the SAXS patterns, which they were able to interpret in terms of distortion of a b.c.c. lattice for the crystalline component of the material. This experiment was performed in the elastic region of the stress–strain curve, and the investigation limited to the SAXS region. Were they to attempt to record the complete WAXS diffraction pattern they would have needed the complete imaging plate to record their image, and an imaging-plate changer would have been required.

In the experiment described in this paper both the WAXS and the SAXS patterns of an elastomer subjected to very large plastic deformations can be recorded on an imaging plate, and the change in structure can be traced through the exposure of a succession of imaging plates carried in

an imaging-plate changer. This is the first time that such a study has been attempted for this class of polyurethane polymers, and the results of the experiment show that their structure–stress relation is completely different from what is usually expected from polymeric systems.

The chief limitation of the acquisition of SAXS data is the size and location of the beamstop. The limitation of the repetition rate at which exposures can be taken is the rate at which imaging plates can be fed by the imaging-plate changer. Although the exposure time used in this study was 30 s, exposures as short as 2 s can give high-quality WAXS/SAXS patterns. The imaging-plate change time is typically 60 s. Because of the relative slowness of data acquisition and the time taken to change imaging plates, such systems cannot be used for truly dynamic WAXS/SAXS experiments. What is important is that the exposure time and the frame rate should be short in comparison with any relaxation processes that might be taking place. Provided these criteria can be met the experimental equipment described here is capable of producing much valuable data on the relation between strain and structure in polymeric systems, especially systems subjected to extremely large strains.

The elastomers used in this study are polyurethane linear segmented co-polymers with an $[HS]_n$-type structure (Martin, Meijs, Renwick, Gunatillake & McCarthy, 1996). These materials usually consist of a relatively flexible component referred to as the soft segment (S) and a relatively polar and stiff component, the hard segment (H). Both hard and soft segments involve sequence length distributions. Micro-domain formation leads to unique elastic properties. The hard domains provide both cross-link sites and filler-like reinforcement of the soft-segment matrix. Conventional X-ray diffractometry using a Siemens 5000 diffractometer in the WAXS region for this class of materials showed two or three relatively broad peaks between 18 and 25° 2θ superimposed on a weak amorphous scattering background centred at $\sim 20°$ 2θ. It is not possible, from these data, to make a quantitative assessment of the crystallite lattice parameters, the crystal structure and the crystallite size.

This paper will demonstrate the increase in resolution achievable using a synchrotron-based imaging-plate system for the characterization of the crystal structure of this class of polyurethane elastomers.

2. Experimental technique

The experiments described in this paper were performed at BL20B at the Photon Factory, KEK, Tsukuba, Japan. A schematic diagram of the beamline and diffractometer is shown in Fig. 1. The monochromator for this system was a fixed-exit-height separated-element double-crystal spectrometer incorporating silicon (111) crystals in which the second crystal can be bent by a four-point bender so as to focus the horizontal beam producing an intensity increase of more than 20 (Creagh & Garrett, 1995). In this experiment the sagittal focusing system was used, and the incident beam size at the specimen position was 35×35 μm. The beam was focused onto the imaging plate.

The specimen was mounted on the θ axis of a unique vacuum diffractometer, the conceptual design for which was due to Wilkins and Creagh (Barnea *et al.*, 1992). The diameter of this diffractometer is in excess of 1 m, and it is possible to mount quite large experimental equipment within it. It was primarily designed for X-ray powder diffraction using imaging plates, but its design is such that a wide variety of experimental configurations, including reflectometry, triple-axis single-crystal diffraction, Bonse–Hart ultra-small-angle scattering *etc.*, can be performed on it with a minimum of setting-up time.

The tensometer was constructed using a Newport 50 mm travel linear slide which was driven by a Newport 850B linear actuator with 50 mm travel. This has a DC motor-encoder which has a positioning accuracy of 0.1 μm and is controlled by the SPEC software used by the diffractometer

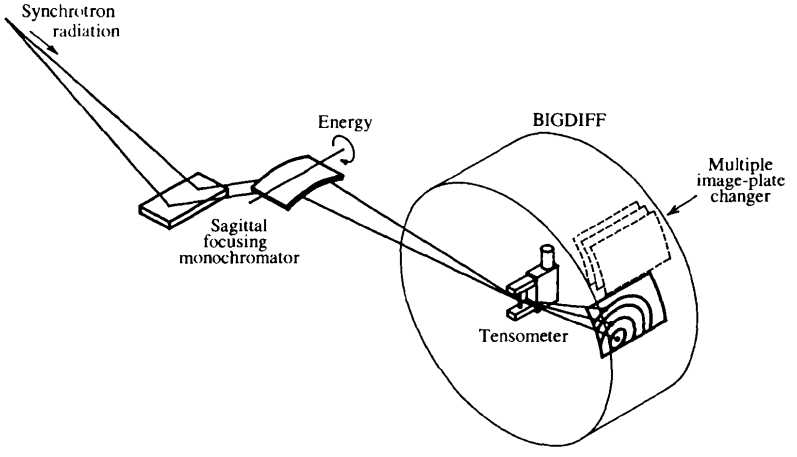

Figure 1
Schematic diagram of the experimental arrangement used, showing the sagittal focusing of the beam, the alignment of the specimen and tensometer with respect to the incident beam and the imaging-plate changer.

system. Specially shaped jaws were fabricated to hold the dumbbell-shaped test specimens. These had typical dimensions 12 × 2 × 0.33 mm. The maximum rate of drawing was 0.4 mm s^{-1}, which corresponds to a maximum strain rate of 10% s^{-1}.

The experiments were conducted at the wavelength of the first peak of the X-ray absorption near-edge structure spectrum of iron, namely 1.7390 Å. A beamstop was set in position behind the specimen to prevent the direct beam from damaging the imaging plates on which the X-ray scattering was recorded. This restricted the smallest observable Q value of the SAXS to ~0.02 $Å^{-1}$ (~1.5°). The peak of the SAXS distribution observed in the laboratory occurred at a value of typically 0.04 $Å^{-1}$, which meant that it was difficult to make measurements of the SAXS on the imaging plate because of the limitations posed by the size of the beamstop in this particular experiment. Nevertheless, it was possible to determine the average crystallite size and orientation from the data and to compare these with the results of a laboratory-based SAXS experiment (O'Neill, 1996).

The imaging plates were situated at a distance 303 mm from the specimen, and only the upper-right quadrant (facing the beam) was used to collect data. Up to ten imaging plates could be mounted in the imaging-plate changer (Foran & Gentle, 1997). The image-plate changer was designed for use in grazing-incidence X-ray diffraction experiments involving thin multilayer films and multiple quantum-well and quantum-dot semiconductor wafers (Holt, Brown, Creagh & Leon, 1997). The imaging plates were read using a Fuji BAS 2000 scanner.

In a typical experiment the sample was mounted with zero strain in the tensometer, the length of the specimen being set normal to the beam. The first imaging plate was then set in position and the beam shutter was opened for 30 s and then closed. The next imaging plate was moved into position, the specimen was strained by an amount set by the tensometer software, and another exposure was taken. This procedure was continued for a strain cycle in which the specimen was extended to a strain of 320% and then had the stress relaxed to zero. A typical stress–strain curve for this class of polyurethane elastomers is shown in Fig. 2(*a*).

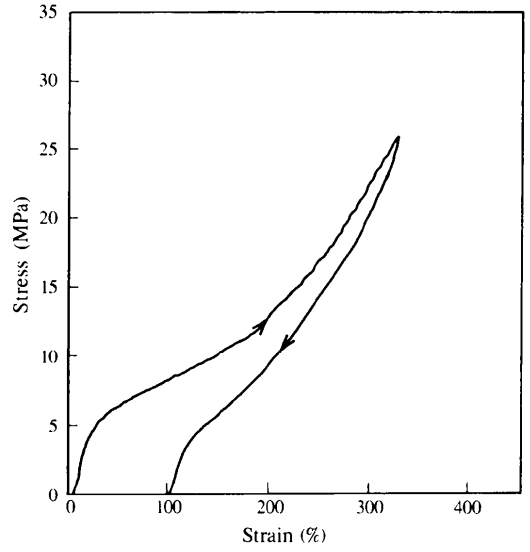

(*a*)

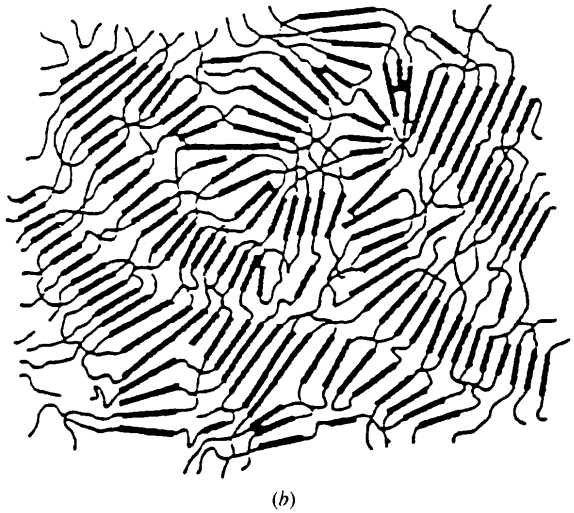

(*b*)

Figure 2
(*a*) A typical stress–strain curve for the class of elastomer used in this study. (*b*) Schematic representation of the polymer system. The parallel sections which correspond to crystallites correspond to aligned hard sections, and the space between the crystallites is filled soft section material.

3. Results

Fig. 3 shows the SAXS/WAXS for a typical loading and unloading sequence. The SAXS/WAXS for an unloaded sample is shown in Fig. 3(*a*). In contrast to the WAXS taken with a conventional laboratory X-ray source the pattern comprises 22 sharp lines, and a number of the Debye rings show that the sample has significant preferred orientation. A complete analysis of the diffraction pattern has not been completed, but it appears to be able to be explained as a slightly distorted centred tetragonal structure. Results of this structural analysis will be reported elsewhere (Creagh, O'Neill & Martin, 1997), together with data from subsequent experiments. It is believed that further measurements on this system will give sufficient information for a structural model of the elastomer to be developed. Of note is the almost complete lack of amorphous background scatter, indicating fully developed crystallites with particles typically ~25 Å in size and the disordered matter is located within the grain boundaries. The crystallites are formed by the juxtaposition of hard segment elements and the regions between the crystallites contain the soft segments. These are tightly coiled and considerable mechanical energy has to be supplied to change their configuration. A schematic diagram of the polymer system is shown in Fig. 2(*b*).

As the strain is increased to about 50% the behaviour is quasi-elastic, in that there is a small amount of hysteresis

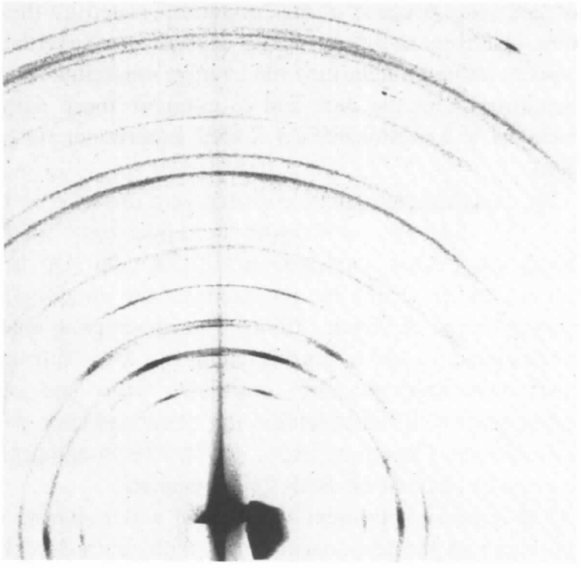

(*a*)

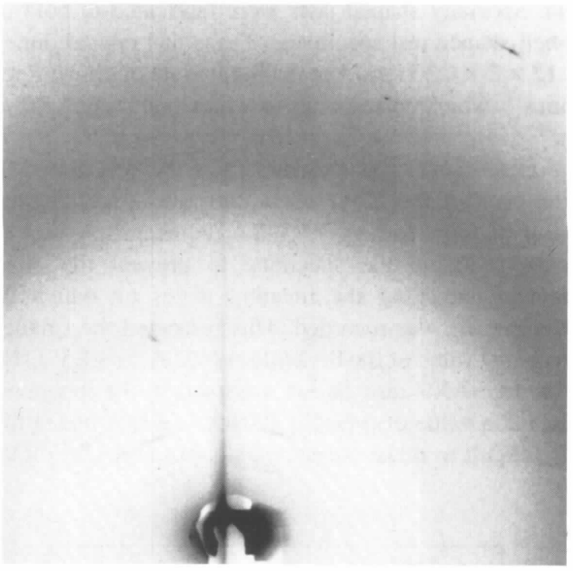

(*b*)

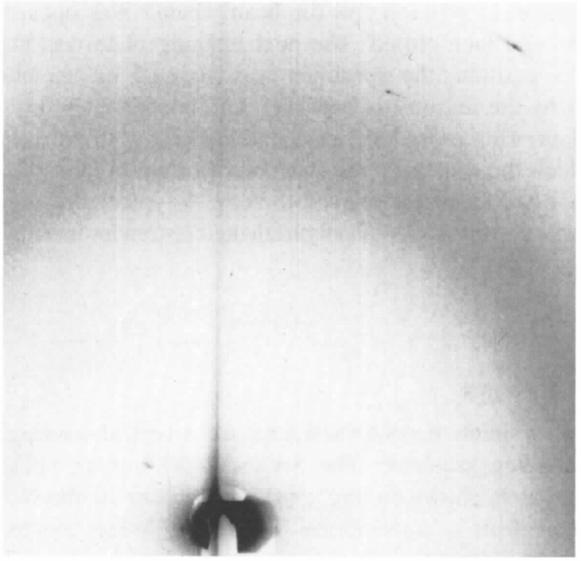

(*c*)

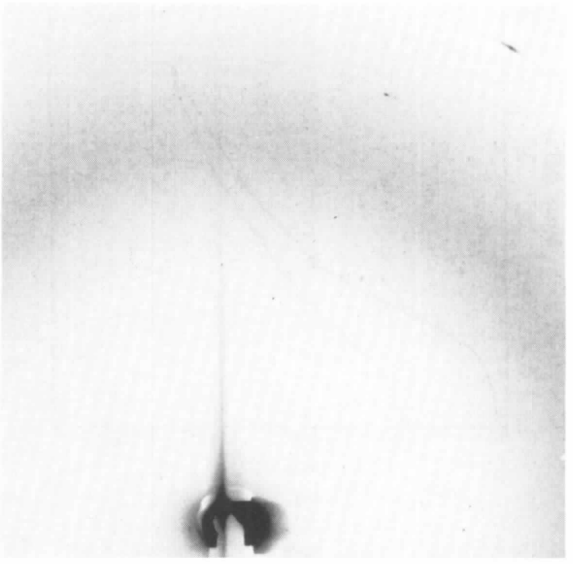

(*d*)

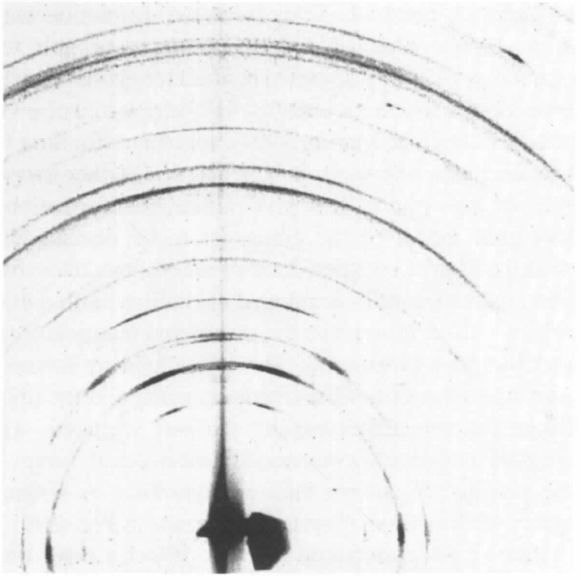

(*e*)

Figure 3
SAXS/WAXS for the elastomer at (*a*) 0%, (*b*) 80%, (*c*) 120%, (*d*) 240% strain and (*e*) at zero applied stress, after straining to 320%.

in the stress–strain graph. This corresponds to the initial region of the stress–strain curve in Fig. 2(*a*). This may be interpreted as a stretching of the polymer links between the crystallites: little change occurs in the crystal structure or distribution of crystallite orientation.

Above 50% strain the slope of the stress–strain curve changes, and the elastic constant drops to less than half its former value. Fig. 3(*b*) shows the diffraction pattern at 80% strain. Some of the inner diffraction lines still exist, and some preferred orientation still remains. The outermost rings, which correspond to the smaller *d* spacings, have broadened to the extent that they give the effect of an amorphous scattering halo.

At 120% strain (Fig. 3*c*) the inner rings have almost disappeared and there is only the faintest hint of them remaining as an amorphous scattered intensity. There is another change of slope in the stress–strain curve, and the elastic modulus increases substantially by about 50%. The crystallites have been unravelled during this phase of the tensile testing.

As the strain increases the trend is more and more towards disorder in the system, and the X-ray scattering distribution is characteristic of an amorphous scatterer. At 240% strain only the outer halo can be seen, and at 320% this halo is both broadened and weakened (Fig. 3*d*). A distribution of voids is produced in these highly strained specimens and can be observed by optical light scattering.

Unloading the specimen reverses the sequence of observations. Crystallinity is once more observed when the specimen is under less than 50% strain, and is fully recovered when the sample is fully unloaded (Fig. 3*e*), although considerable permanent deformation has occurred. Preliminary studies show that subsequent loading/unloading sequences give results similar to the initial loading/unloading sequence, with the same development from an ordered to a disordered system being observed.

After about two months the specimens relax to have very nearly the same dimensions as they had initially. The voids also disappear. Both of these observations indicate that strong relaxation mechanisms are at work in these polyurethane polymers.

4. Conclusions

Whilst other SAXS/WAXS systems have been devised for the study of elastomers, the low background afforded by the operation of the tensometer in a vacuum diffractometer, and the resolution and sensitivity of the imaging-plate system, makes the equipment described in this paper unique. Its angular range of measurement is potentially from 0.5 to 30°. The angular resolution of the system is 0.03°. The system described here is a prototype system and a number of modifications will be made to it and to our operating procedures for our next allocated beam time, namely:

(i) the beamstop will be redesigned and repositioned;

(ii) a load cell will be mounted on the linear slide so that the complete stress–strain curve can be acquired during the loading/unloading sequence;

(iii) modifications will be made to the mount on which the tensometer attaches to the θ axis, to enable more exact positioning of the specimen in the beam;

(iv) the strain rate will be increased to 200% s^{-1};

(v) the exposure time will be reduced to 2 s to assist in the study of the crystalline segment of the stress–strain curve, and the study of stress relaxation.

The tensile behaviour of the polyurethane elastomers studied here is different from that usually observed for polymers, and these are the first experiments of this type performed on this class of materials. We will make further experiments to examine the effect of strain rate and relaxation.

A summary of our observations is as follows:

(i) the elastomer is almost crystalline in its original unstrained state, with the structural disorder within the crystallites associated with the soft segments of the polymer;

(ii) the elastomer possesses a high degree of preferred orientation which is induced when the specimen is cast;

(iii) the crystallites contain the hard section components, and the grain boundaries contain the soft segments;

(iv) for strains less than 50% the behaviour is quasi-elastic, and the fact that the characteristics of the diffraction pattern do not change in this range of strains leads to the conclusion that the initial stage of the stress–strain curve is associated with processes taking place within the grain boundaries and not to changes within the crystallites;

(v) for strains greater than 50% no further extension of the material within the grain boundaries is possible and the crystallites start to unravel, and the cross-links between hard segment chains become increasingly misaligned, leading to a destruction of the crystalline order of the elastomer;

(vi) for strains in excess of 160% the elastomer becomes increasingly disordered, and the extension can only occur through changes in the configuration of the polymer chains;

(vii) at maximum strain only the radial distribution function of the average electron density of the elastomer is observed, indicating that the elastomer has become very highly disordered.

We are indebted to the Australian National Beamline Facility which provided funding for this study, and to the Australian Nuclear Science and Technology Organization which administers the Access to Major Facilities Program.

References

Barnea, Z., Creagh, D. C., Davis, T. J., Grigg, M., Stephenson, A. W. & Wilkins, S. W. (1992). *Rev. Sci. Instrum.* **63**, 1069–1072.

Bras, W., Mant, A. J., Derbyshire, G. E., O'Kane, W. J., Helsby, W. I., Hall, C. J. & Ryan, A. J. (1995). *J. Synchrotron Rad.* **2**, 87–92.

Butler, M. F., Donald, A. M., Bras, W., Mant, G. R., Derbyshire, G. E. & Ryan, A. J. (1995). *Macromolecules*, **28**, 6383–6393.

Creagh, D. C. & Garrett, R. F. (1995). *Access to Major Facilities Program*, edited by J. W. Boldeman, pp. 251–252. ANSTO, Sydney, Australia.
Creagh, D. C., O'Neill, P. M. & Martin, D. J. (1997). *J. Appl. Polym. Sci.* In preparation.
Foran, G. J. & Gentle, I. A. (1997). *Langmuir*. In the press.
Holt, S. A., Brown, A. S., Creagh, D. C. & Leon, R. (1997). *J. Synchrotron Rad.* **4**, 168–173.
Hughes, D. J., Mahendrasingam, A., Heeley, E. L., Oatway, W. B., Martin, C. & Fuller, W. (1996). *J. Synchrotron Rad.* **3**, 84–90.
Martin, D. J., Meijs, G. P., Renwick, G. M., Gunatillake, P. A. & McCarthy, S. J. (1996). *J. Appl. Polym. Sci.* **60**, 557–571.
O'Neill, P. M. (1996). Thesis, University College, The University of New South Wales, Australia.
Suehiro, S., Saijo, K., Seto, T., Sakamoto, N., Hashimoto, T., Ito, K. & Amemiya, Y. (1996). *J. Synchrotron Rad.* **3**, 225–230.